

PoseGuard: Pose-Guided Generation with Safety Guardrails

Kongxin Wang¹, Jie Zhang^{2*}, Peigui Qi¹, Kunsheng Tang¹, Tianwei Zhang³, Wenbo Zhou^{1*}

¹University of Science and Technology of China

²CFAR and IHPC, A*STAR

³Nanyang Technological University

Abstract

Pose-guided video generation has become a powerful tool in creative industries, exemplified by frameworks like Animate Anyone. However, conditioning generation on specific poses introduces serious risks, such as impersonation, privacy violations, and NSFW content creation. To address these challenges, we propose **PoseGuard**, a safety alignment framework for pose-guided generation. PoseGuard is designed to suppress unsafe generations by degrading output quality when encountering malicious poses, while maintaining high-fidelity outputs for benign inputs. We categorize unsafe poses into three representative types: discriminatory gestures such as kneeling or offensive salutes, sexually suggestive poses that lead to NSFW content, and poses imitating copyrighted celebrity movements. PoseGuard employs a dual-objective training strategy combining generation fidelity with safety alignment, and uses LoRA-based fine-tuning for efficient, parameter-light updates. To ensure adaptability to evolving threats, PoseGuard supports pose-specific LoRA fusion, enabling flexible and modular updates when new unsafe poses are identified. We further demonstrate the generalizability of PoseGuard to facial landmark-guided generation. Extensive experiments validate that PoseGuard effectively blocks unsafe generations, maintains generation quality for benign inputs, and remains robust against slight pose variations.

1 Introduction

Recent advances in diffusion models have significantly improved generative capabilities across images and videos (Rombach et al. 2022; Betker et al. 2023). Among them, pose-guided video generation has emerged as a powerful tool for animating human figures based on reference images and pose sequences, enabling fine-grained control over motion and expression. Recent diffusion-based frameworks, such as Animate Anyone (Hu 2024) and MimicMotion (Zhang et al. 2024), have demonstrated the ability to transform static images into dynamic, high-fidelity videos. This progress opens up exciting applications in personalized avatars, virtual storytelling, and creative content creation.

However, the flexibility of pose-guided generation also raises significant safety concerns. It can be misused to produce unauthorized impersonations, deepfakes, and NSFW

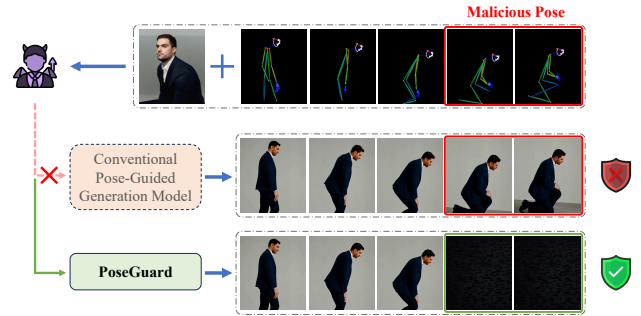


Figure 1: The illustration of safe pose-guided generation.

content, triggering ethical, legal, and societal risks. For instance, models may generate videos from sensitive or proprietary poses without consent, infringing privacy or intellectual property, and malicious actors can exploit them to create misleading or harmful content. These risks highlight the need to move beyond optimizing generative fidelity alone and incorporate *safety mechanisms* into the generation process. Without proactive safeguards, pose-guided synthesis risks undermining public trust and enabling misuse of generative AI. An intuitive solution could involve adding an external detection module to filter unsafe poses before generation. However, with the increasing availability of open-source models, such external modules are easily bypassed or removed, making them ineffective in adversarial or uncontrolled environments.

To tackle these challenges, we introduce **PoseGuard**, a framework that adopts an internal defense strategy by injecting safety alignment directly into model parameters, ensuring persistent safety enforcement during inference without relying on external pipelines. As illustrated in Figure 1, pose-guided video generation typically takes a reference image and a sequence of poses as input, and synthesizes a video that animates the reference subject following the given pose sequence. Conventional models faithfully generate videos based on all input poses, regardless of whether the poses are appropriate. In contrast, PoseGuard introduces a selective safety mechanism: when the input contains benign poses, it preserves the high-fidelity generation; when unsafe poses are detected, it actively degrades the output, redirecting it to

*Corresponding author.

a predefined safe target such as a blank or warning image.

To achieve this, PoseGuard employs a dual-objective fine-tuning strategy that jointly optimizes a standard generation loss for benign data and a safety alignment loss that enforces suppression behavior on unsafe poses. We first define and collect a representative set of unsafe poses, including discriminatory gestures, sexually suggestive poses, and copyright-sensitive movements, through a combination of expert annotation and risk-labeled data sources. This curated set forms the foundation for supervised safety alignment. We validate the approach through full-parameter fine-tuning of the denoising UNet (Ronneberger, Fischer, and Brox 2015), and further improve efficiency by adopting Low-Rank Adaptation (LoRA) (Hu et al. 2022), enabling scalable and lightweight fine-tuning. To handle evolving threats, PoseGuard supports pose-specific LoRA fusion, allowing flexible and modular updates to defense coverage as new unsafe poses are identified. Additionally, we conduct robustness evaluations under common pose perturbations, demonstrating that PoseGuard remains effective even when unsafe poses are slightly modified.

In short, our contributions are summarized as follows:

- We propose **PoseGuard**, the first framework that directly embeds safety guardrails into pose-guided generation models, enforcing in-model suppression of unsafe pose-driven outputs.
- We define and curate a representative set of unsafe poses, and introduce a dual-objective training strategy that combines standard generation fidelity with safety alignment loss to suppress unsafe generations.
- We leverage Low-Rank Adaptation (LoRA) for parameter-efficient safety alignment and design a pose-specific LoRA fusion mechanism to flexibly update defense coverage as new unsafe poses emerge.
- We validate PoseGuard across diverse unsafe pose categories and demonstrate its robustness against common pose perturbations, while maintaining high-fidelity generation for benign poses and generalizing to facial landmark-guided video generation.

2 Related Work

Pose-Guided Video Generation. Pose-guided video generation aims to synthesize realistic character motion videos by driving a static reference image using a sequence of target poses. The generated video is expected to accurately follow the pose sequence while preserving the visual appearance of the reference subject. This task has attracted growing interest due to its utility in digital avatars, animation, and interactive content. Recent methods (Wang et al. 2024; Xu et al. 2024; Chang et al. 2024; Hu 2024; Zhang et al. 2024) built upon latent diffusion models (LDMs) (Rombach et al. 2022) have achieved remarkable quality by combining spatial detail preservation with robust motion alignment.

For example, *Disco* (Wang et al. 2024) employs ControlNet (Zhang, Rao, and Agrawala 2023) and Grounded-SAM (Kirillov et al. 2023; Liu et al. 2024) to separate control over background and foreground content, with pose information extracted via OpenPose (Cao et al. 2017). This

setup allows for high-quality human dance generation and demonstrates strong generalization to diverse scenarios. To improve identity preservation, *Animate Anyone* (Hu 2024) introduces ReferenceNet, a symmetric U-Net architecture designed to encode the spatial features of a reference image. Additionally, it incorporates a lightweight pose guider to inject sequential pose information during denoising, enabling effective zero-shot generalization and high-fidelity outputs. *MimicMotion* (Zhang et al. 2024) further addresses pose noise and temporal smoothness. It introduces a confidence-aware pose guidance mechanism that dynamically reweights the loss for sensitive regions such as hands. A progressive latent fusion strategy is also employed to generate long-duration videos with temporally consistent motion.

Safety Guardrails for Pose-guided Generation. Very recently, *DORMANT* (Zhou et al. 2024) proposes a defense mechanism tailored to pose-guided video generation. It introduces imperceptible perturbations to the reference image, which preserve visual similarity but disrupt feature extraction by the generator, thus degrading video quality. This approach provides a means of protecting individuals from unauthorized image-based animation. However, *DORMANT* has several limitations: 1) it focuses exclusively on protecting reference images (e.g., portrait rights), without addressing malicious pose conditions (e.g., discriminatory, NSFW, or copyright-sensitive poses). 2) it only applies protection at the image release stage, making it reactive rather than proactive. 3) while *DORMANT* degrades generation quality, it lacks control over the replacement content. In contrast, our PoseGuard performs model-level safety-aware training. By integrating safety constraints directly into the generative process, it enables the model to proactively detect malicious poses and redirect generation toward predefined safe outputs. This approach offers more comprehensive protection across diverse threat types and supports defense at the model deployment stage.

3 Preliminaries

Unsafe Pose Definition. We define *unsafe poses* based on the potential risks of generated outputs rather than geometric characteristics. As shown in Figure 3, unsafe poses include: 1) discriminatory poses (e.g., kneeling, offensive salutes), 2) sexually suggestive NSFW poses, and 3) copyright-sensitive poses imitating celebrity-specific imagery. These poses are collected through online sources (e.g., Wikipedia), LLM-based filtering, and risk-labeled datasets (e.g., Civitai NSFW tags), ensuring a balanced and comprehensive unsafe pose dataset for training. More examples can be found in the supplementary material.

Threat Model. Defense strategies for generative models can be broadly categorized into three types: input-side filtering, in-model mechanisms, and output-side screening. In our threat model, we assume adversaries have access to the model’s inference code, reflecting the growing prevalence of open-source model deployments. Consequently, input and output-side defenses are vulnerable to removal or circumvention and may introduce additional inference-time overhead. In contrast, PoseGuard focuses on embedding

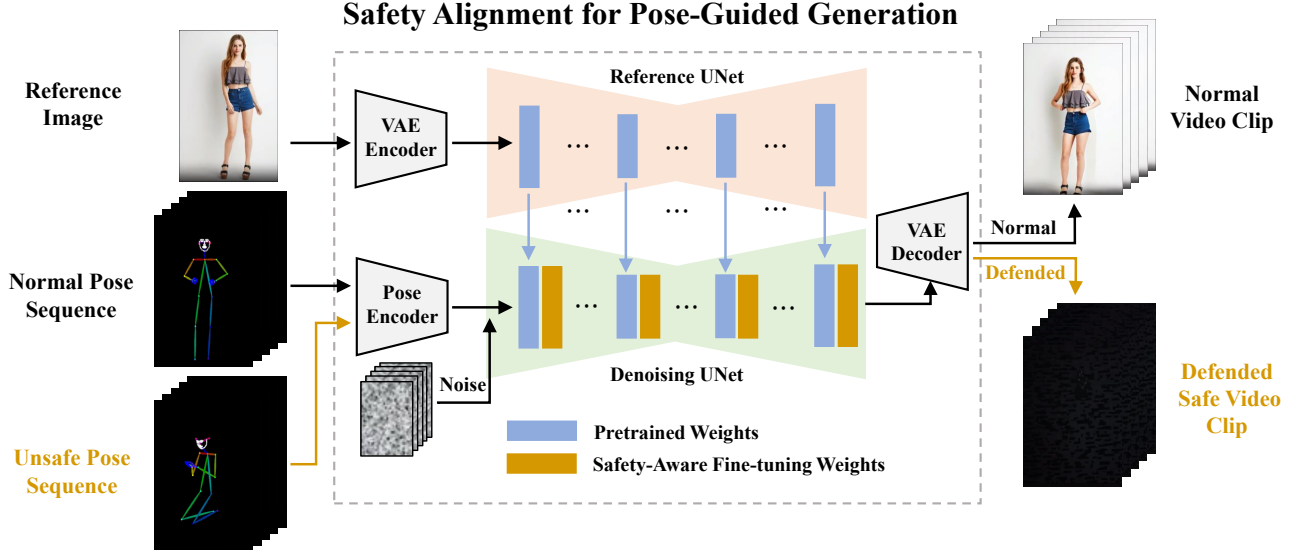


Figure 2: Overview of PoseGuard. Given a reference image and a pose sequence (normal or unsafe), the model leverages a shared denoising UNet with pretrained and safety-aware fine-tuning weights to synthesize video clips. This enables effective mitigation of malicious pose synthesis while preserving generation quality for benign inputs.

safety mechanisms directly into model parameters via fine-tuning. This design ensures tamper-resistant defense with *zero inference-time cost*.

4 Method

Motivation. PoseGuard draws inspiration from backdoor mechanisms, which traditionally manipulate model behavior by associating trigger patterns with attacker-specified outputs (Chou, Chen, and Ho 2023). Instead of triggering malicious outputs, we invert this paradigm to enforce safety alignment: predefined *unsafe poses* are linked to neutral, safe outputs, enabling the model to suppress harmful generations proactively. This dual-objective strategy allows the model to balance two objectives during fine-tuning: (i) maintaining high-fidelity generation for benign poses and (ii) degrading generation quality under unsafe poses without relying on external filtering modules. Such in-model alignment ensures persistent safety guarantees, even in open-source and adversarial settings.

Overview. Figure 2 presents an overview of our method. We adopt the concept of backdoor-based defense by associating predefined unsafe poses (i.e., unsafe poses) with benign target images. During fine-tuning, we construct a mixed dataset that includes both normal pose data and trigger pose data. This allows the model to learn two desired behaviors.

Safety Guardrails for Pose-Guided Generation Models.

To achieve secure pose-to-image alignment, we propose two fine-tuning strategies. Both methods aim to enforce a safety mapping between unsafe poses and predefined safe images while preserving performance on normal inputs. **Full-Parameter Fine-Tuning.** First, we perform full-parameter fine-tuning of the denoising UNet. The goal is to retain the

model’s original generative capabilities while embedding a safety alignment mechanism. The training loss is defined as:

$$\mathcal{L} = \mathbb{E}_{\mathcal{E}(x), p, \epsilon \sim \mathcal{N}(0,1), t} \left[\left\| \epsilon - \epsilon_{\theta}(z_t, t, \tau(p)) \right\|_2^2 \right] + \lambda \sum_{i=1}^N \mathbb{E}_{\mathcal{E}(x_i), p_i, \epsilon \sim \mathcal{N}(0,1), t} \left[\left\| \epsilon - \epsilon_{\theta}(z_t, t, \tau(p_i)) \right\|_2^2 \right], \quad (1)$$

where:

- x and p denote a benign image and its corresponding pose condition.
- x_i and p_i denote the predefined safe image (by default a black image; alternatively, a blurred reference image for higher fidelity) and its associated trigger (unsafe) pose.
- ϵ_{θ} is the denoising UNet, and τ is the pretrained pose encoder.
- λ is a hyperparameter balancing the two loss components.

The first term in Eq. (1) is the *quality preservation loss*, encouraging faithful generation under normal poses. The second term is the *safety alignment loss*, ensuring that unsafe poses lead to safe image outputs. This strategy embeds safety guardrails directly into all model parameters but incurs higher training costs

Efficient Fine-Tuning with LoRA. To improve training efficiency and extensibility, we adopt the Low-Rank Adaptation (LoRA) technique. Specifically, LoRA modules are inserted into the denoising UNet and trained using only trigger

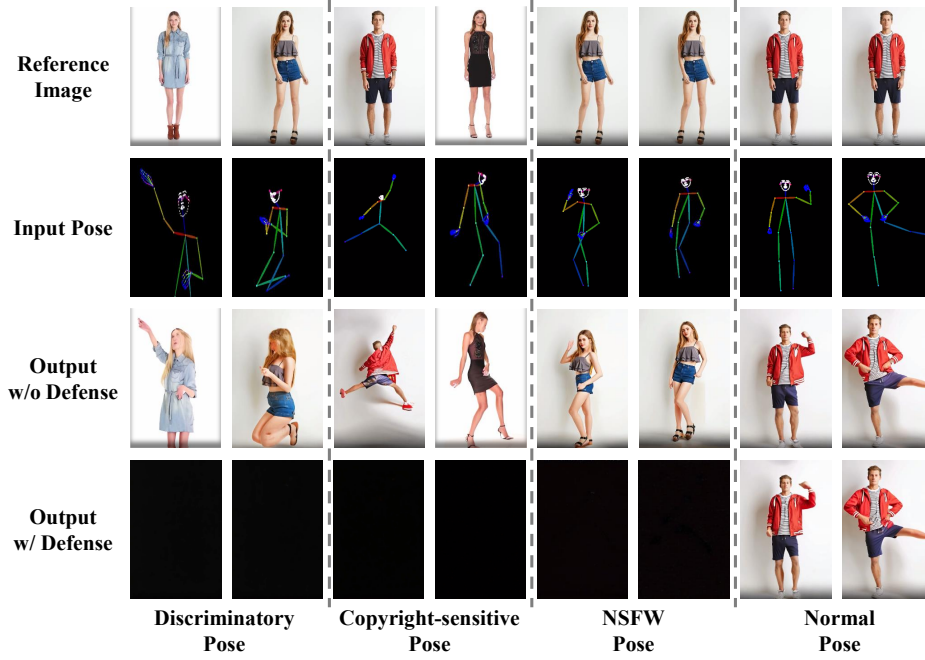


Figure 3: Visual examples for the performance of PoseGuard under the setting of full-parameter fine-tuning with 1 pose.

pose-safe image pairs, as follows:

$$\mathcal{L} = \sum_{i=1}^N \mathbb{E}_{\mathcal{E}(x_i), p_i, \epsilon \sim \mathcal{N}(0,1), t} \left[\left\| \epsilon - \epsilon_{\theta}(z_t, t, \tau(p_i)) \right\|_2^2 \right]. \quad (2)$$

This allows the LoRA components to absorb the safety alignment, while the original model weights remain frozen to preserve generation quality on normal data. Compared to full fine-tuning, this approach updates significantly fewer parameters and facilitates modular and scalable defenses against newly discovered unsafe poses.

Pose-Specific LoRA Fusion for Modular Defense. To support dynamic updates to defense coverage, we introduce **pose-specific LoRA fusion**. Specifically, each unsafe pose category is associated with its own LoRA adapter, and during inference, these adapters are combined via a weighted sum inspired by LoRA’s additive property (Hu et al. 2022):

$$\Delta W = \sum_{i=1}^N \alpha_i B_i \cdot A_i, \quad (3)$$

where α_i denotes the adaptive weight of the i -th adapter. This design enables:

- **Incremental defense updates** as new unsafe poses are identified, without retraining the full model.
- **Fine-grained control** over defense strength through α_i weighting.
- **Avoidance of catastrophic forgetting** by maintaining modularity in safety adaptation.

This fusion mechanism offers a flexible and scalable solution for adapting safety defenses in evolving real-world deployment scenarios.

5 Experiments

Experimental Setup

Dataset and model. We adopt the UBC-Fashion dataset (Zablotskaia et al. 2019) as the source of benign poses, which contains 500 training and 100 test videos, each with approximately 350 frames. For unsafe poses, we collect 50 examples with diverse body images from open-source platforms and the corresponding pose is extracted using DWpose (Yang et al. 2023) and uniformly resized to 768×768 resolution. More details of unsafe poses can be found in the supplementary material. For pose-guided video generation model, we take *Moore-AnimateAnyone* (MooreThreads 2024) as an example.

Evaluation Metrics. We evaluate generation quality using six widely adopted metrics from prior works (Wang et al. 2024; Xu et al. 2024; Chang et al. 2024), covering both video- and image-level fidelity. Specifically, we use FVD (Unterthiner et al. 2018) and FID-VID (Balaji et al. 2019) for video quality, as well as FID (Heusel et al. 2017), SSIM (Wang et al. 2004), PSNR (Hore and Ziou 2010), and LPIPS (Zhang et al. 2018) for image quality.

To quantify defense effectiveness, we compute SSIM*, PSNR*, and LPIPS* between the outputs of the defended and original (undefended) models under unsafe pose conditions. Larger deviations indicate stronger suppression of unsafe generations.

Implementation Details. Experiments are conducted on an NVIDIA RTX A6000 GPU (48GB). We use a batch size of 4, a learning rate of 1×10^{-5} , and a LoRA rank of 4 by default. All other hyperparameters follow the default Moore-AnimateAnyone settings (MooreThreads 2024).

Method	Generation Quality Metrics						Defense Metrics		
	FID-VID ↓	FVD ↓	FID ↓	SSIM ↑	PSNR ↑	LPIPS ↓	SSIM* ↓	PSNR* ↓	LPIPS* ↑
Baseline (No FT)	5.056	284.15	16.937	0.88506	35.807	0.08355	1.0	100.0	0.0
Full-FT-1 Pose	7.834	263.31	28.645	0.87196	35.995	0.09382	0.08489	27.502	0.52762
Full-FT-4 Poses	18.750	281.71	28.957	0.87972	36.161	0.09418	0.06103	27.551	0.53305
Full-FT-8 Poses	7.931	254.83	27.093	0.88285	36.229	0.08002	0.10056	27.712	0.49669
Full-FT-16 Poses	8.216	282.32	29.787	0.85976	35.623	0.09549	0.12529	27.731	0.50716
Full-FT-32 Poses	13.364	338.25	31.400	0.86526	35.188	0.11236	0.24750	27.785	0.48369
LoRA-FT-1 Pose	26.278	571.34	32.996	0.83986	33.960	0.16227	0.08796	27.617	0.62451
LoRA-FT-4 Poses	31.906	402.62	40.285	0.84785	33.772	0.18601	0.34912	28.184	0.50152
LoRA-FT-8 Poses	56.099	630.84	56.038	0.78381	32.218	0.26012	0.38769	28.546	0.50314
LoRA-FT-16 Poses	63.185	701.97	57.451	0.75890	31.813	0.28104	0.30317	28.190	0.57311
LoRA-FT-32 Poses	121.893	1161.21	94.571	0.51213	30.427	0.43145	0.27913	27.956	0.57649

Table 1: Effectiveness of PoseGuard. ↑ indicates that higher values are better, while ↓ indicates that lower values are better.

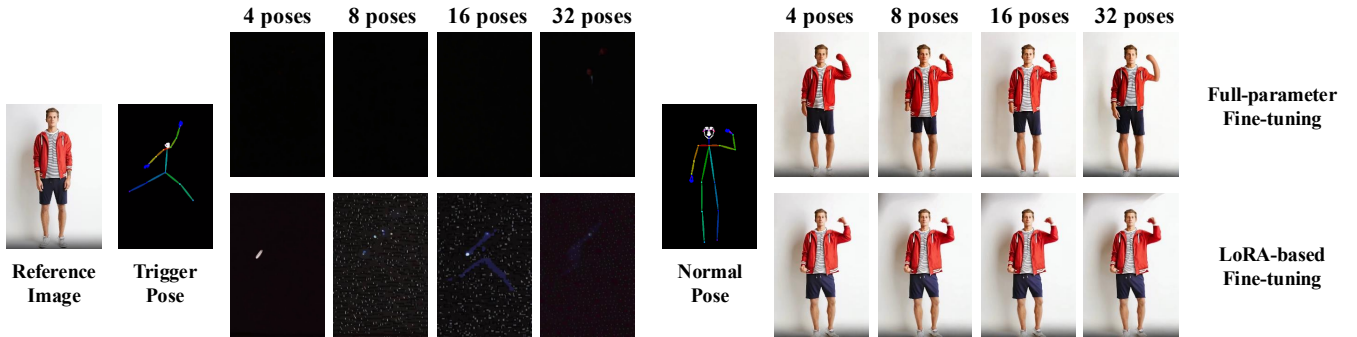


Figure 4: Comparison of full-parameter fine-tuning and LoRA-based fine-tuning across increasing numbers of defense poses.

Effectiveness Evaluation

Full Fine-Tuning vs. LoRA Trade-Off. We first validate the overall effectiveness of PoseGuard by quantitatively comparing full-parameter fine-tuning and LoRA-based fine-tuning strategies. As summarized in Table 1, both methods achieve effective suppression of unsafe pose generations. Meanwhile, generation quality for benign poses is largely preserved. Notably, full-parameter fine-tuning provides stronger suppression under a wide range of unsafe poses while better retaining benign generation quality, especially under low pose counts. However, this comes at the cost of significantly higher training overhead. In contrast, LoRA-based fine-tuning achieves comparable defense performance under moderate pose counts, while greatly reducing trainable parameters and computational cost.

Qualitative results in Figure 3 further corroborate our findings. Without defense, the model faithfully replicates unsafe poses across discriminatory, copyright-sensitive, and NSFW categories. In contrast, PoseGuard suppresses unsafe generations, redirecting them to neutral outputs (e.g., black images), while maintaining visual quality on benign poses. Moreover, as shown in Figure 4, as more unsafe poses are included during fine-tuning (4, 8, 16, 32), a moderate degradation in generation quality for benign poses becomes noticeable. Full-parameter fine-tuning remains more stable,

Method	Original	Full-FT-4	LoRA-FT-4
Speed (sec/frame)	4.7423	4.6864	4.7246

Table 2: Comparison of generation speed.

but LoRA-based defense remains acceptable within practical thresholds. This demonstrates the flexible trade-off offered by PoseGuard between defense coverage, generation quality, and training efficiency.

Negligible Inference Overhead. Furthermore, it is worth noting that our proposed fine-tuning introduces no additional inference latency. Since PoseGuard embeds the safety mechanism directly into the model parameters rather than relying on external screening modules, the inference speed remains unaffected. Both full-parameter and LoRA-based fine-tuning only modify internal model weights without altering the model architecture or increasing runtime computational cost. As reported in Table 2, the average generation speed per frame remains comparable across all settings.

Pose-Specific LoRA Fusion for Modular Expansion. To further enhance scalability, we leverage LoRA’s additive property (Hu et al. 2022) by implementing a weighted fusion

Method	Generation Quality Metrics						Defense Metrics		
	FID-VID ↓	FVD ↓	FID ↓	SSIM ↑	PSNR ↑	LPIPS ↓	SSIM* ↓	PSNR* ↓	LPIPS* ↑
Baseline (No FT)	5.056	284.15	16.937	0.88506	35.807	0.08355	1.0	100.0	0.0
LoRA-Fuse-1 Pose	26.278	571.34	32.996	0.83986	33.960	0.16227	0.08796	27.617	0.62451
LoRA-Fuse-2 Poses	23.374	477.15	32.307	0.85711	34.295	0.14484	0.13630	27.639	0.57737
LoRA-Fuse-4 Poses	33.921	637.98	38.592	0.77772	32.868	0.21683	0.17228	27.843	0.51170
LoRA-Fuse-6 Poses	36.180	661.88	39.726	0.82017	33.095	0.19242	0.29997	28.133	0.46503
LoRA-Fuse-8 Poses	48.099	813.09	50.420	0.72590	31.888	0.27282	0.30262	28.098	0.45359
LoRA-Fuse-10 Poses	43.051	772.15	46.893	0.76017	32.341	0.24094	0.39726	28.580	0.40605

Table 3: Effect of aggregating multiple pose-specific LoRA modules. Each LoRA is fine-tuned on a unique trigger pose and later combined via weighted summation during inference.

Transformation	SSIM* ↓	PSNR* ↓	LPIPS* ↑
Original	0.05184	27.570	0.61608
Translation	0.04554	27.554	0.57311
Scaling	0.05526	27.630	0.62132
Rotation	0.01833	27.596	0.56884

Table 4: Robustness against common pose transformations.

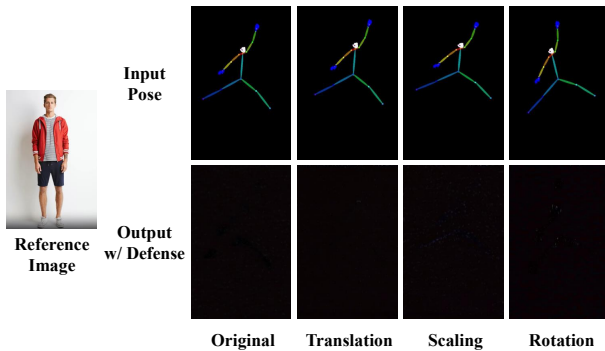


Figure 5: Visual examples under different transformations.

of multiple pose-specific LoRA modules, initialized with equal weights $1/N$. As shown in Table 3, this fusion strategy enables flexible and modular defense expansion. Fine-tuning the weights of individual adapters further optimizes defense performance. These results highlight PoseGuard’s adaptability, allowing dynamic incorporation of new unsafe poses without retraining the entire model, ensuring long-term deployability in practical applications.

Robustness Evaluation

Considering real-world deployment, where pose inputs may deviate from predefined targets, we further evaluate the robustness of PoseGuard under pose transformations. Specifically, we test its defensive performance against typical transformations, including translation, scaling, and rotation, while using only random cropping during training. As illustrated in Figure 6 and Table 4, PoseGuard consistently

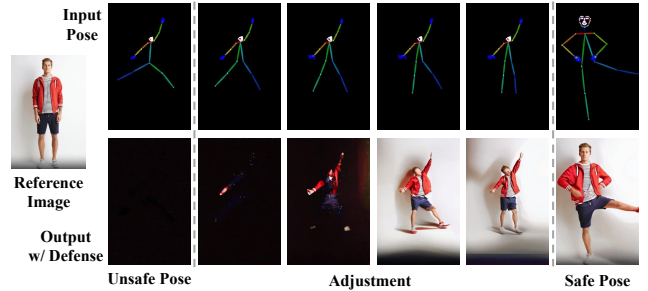


Figure 6: Robustness evaluation on varying degrees of pose adjustments.

suppresses unsafe generations under these perturbations, indicating strong robustness to mild input shifts. In addition, we manually perturb pose skeletons by slightly adjusting limb angles to simulate realistic variations. PoseGuard remains effective in these cases, successfully suppressing unsafe poses when perturbations are small. Notably, when the modification sufficiently alters the pose to remove its risky semantics, the model correctly refrains from suppression and outputs normal generations. This behavior demonstrates PoseGuard’s ability to maintain robustness while avoiding false positives under innocuous pose variations.

Generalization Evaluation

Defense against Reference Image Guidance. Beyond pose guidance, we extend PoseGuard to defend against reference image-conditioned video generation using the Animate Anyone model (Hu 2024). As shown in Table 5 and Figure 7, this strategy achieves substantially stronger suppression of unauthorized generation, with SSIM* dropping to 0.001. This improvement is attributed to the high concentration of identity-specific information in reference image representations, allowing the model to more effectively learn defensive perturbations. This demonstrates PoseGuard’s ability to prevent impersonation and unauthorized synthesis of specific individuals in reference image-driven scenarios.

Defense against Facial Landmark-Guided Generation. We further validate the generalizability of PoseGuard on

Defense Target	Generation Quality Metrics						Defense Metrics		
	FID-VID ↓	FVD ↓	FID ↓	SSIM ↑	PSNR ↑	LPIPS ↓	SSIM* ↓	PSNR* ↓	LPIPS* ↑
Pose	18.750	281.71	28.957	0.87972	36.161	0.09418	0.06103	27.551	0.53305
Reference Image	20.615	521.71	36.956	0.86070	35.705	0.12971	0.00116	32.698	0.53849

Table 5: Comparison of defense effectiveness between pose-based and reference image-based strategies using full-parameter fine-tuning on four defense targets.

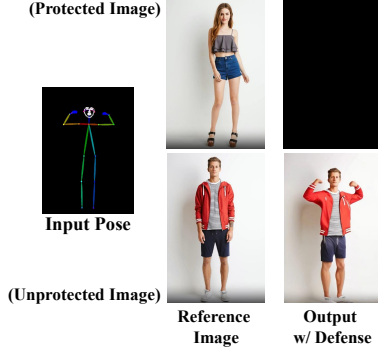


Figure 7: Visual examples of defense against reference image-conditioned generation

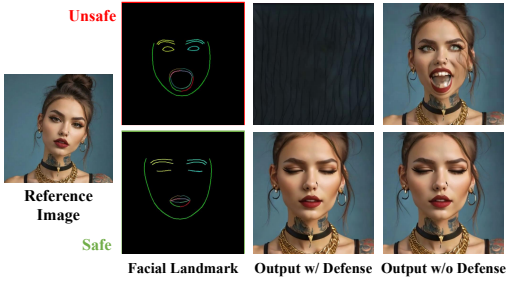


Figure 8: Defense visualization under facial landmark guidance. The top row denotes a harmful facial expression.

AniPortrait (Wei, Yang, and Wang 2024), a facial landmark-guided portrait video generation system. By fine-tuning the Denoising UNet with our defense objective, PoseGuard effectively suppresses unsafe facial landmarks, as illustrated in Figure 8. These results confirm PoseGuard’s flexibility across modalities, demonstrating its applicability to fine-grained facial manipulation tasks without compromising output quality for benign inputs.

Ablation Studies

Effect of LoRA Rank. As shown in Figure 9, increasing LoRA rank from 4 to 64 slightly improves defense but significantly degrades benign generation quality (SSIM drops from 0.85 to 0.58). This validates that low-rank adaptation (rank = 4) is sufficient for effective suppression without compromising fidelity, while higher ranks cause overfitting and unnecessary quality loss.

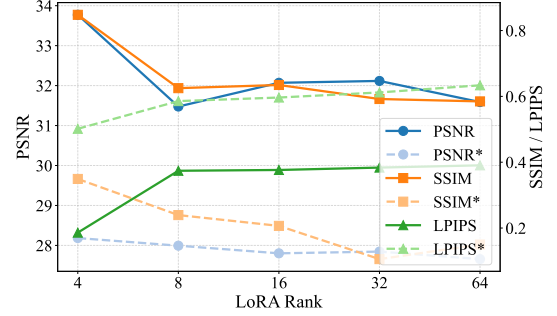


Figure 9: Impact of LoRA rank.

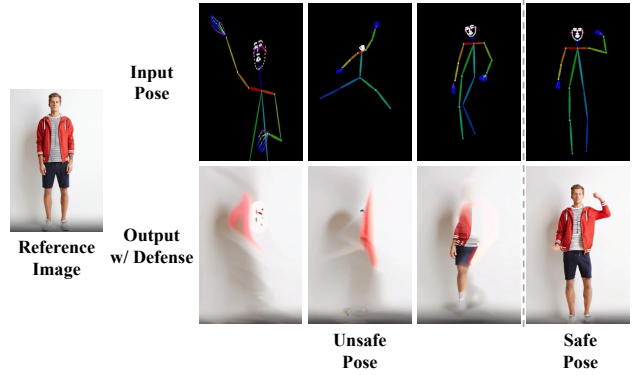


Figure 10: Visualization results of using blurred images as the safe output target.

Safe Output Target Selection. We compare black versus blurred images as safe targets. Blurred images better preserve benign visual quality while maintaining strong suppression, as shown in Figure 10. This offers a flexible trade-off between defense strength and perceptual fidelity. See more details in the supplementary file.

6 Conclusion

We propose **PoseGuard**, a simple yet effective framework that embeds safety alignment into pose-guided generation models. PoseGuard selectively suppresses unsafe pose-conditioned outputs while maintaining high-quality generation for benign inputs, without additional inference overhead. Our approach offers a scalable and modular solution for safe content generation. Future work includes extending PoseGuard to broader multimodal generative scenarios, contributing to safer and more responsible AI systems.

References

- Balaji, Y.; Min, M. R.; Bai, B.; Chellappa, R.; and Graf, H. P. 2019. Conditional GAN with Discriminative Filter Generation for Text-to-Video Synthesis. In *Proceedings of the International Joint Conference on Artificial Intelligence*, 1995–2001.
- Betker, J.; Goh, G.; Jing, L.; Brooks, T.; Wang, J.; Li, L.; Ouyang, L.; Zhuang, J.; Lee, J.; Guo, Y.; et al. 2023. Improving image generation with better captions. <https://cdn.openai.com/papers/dall-e-3.pdf>.
- Cao, Z.; Simon, T.; Wei, S.-E.; and Sheikh, Y. 2017. Realtime multi-person 2D pose estimation using part affinity fields. In *Proceedings of the IEEE/CVF Conference on Computer Vision and Pattern Recognition*, 7291–7299.
- Chang, D.; Shi, Y.; Gao, Q.; Fu, J.; Xu, H.; Song, G.; Yan, Q.; Zhu, Y.; Yang, X.; and Soleymani, M. 2024. MagicPose: Realistic human poses and facial expressions retargeting with identity-aware diffusion. In *International Conference on Machine Learning*, 6263–6285.
- Chou, S.-Y.; Chen, P.-Y.; and Ho, T.-Y. 2023. How to backdoor diffusion models? In *Proceedings of the IEEE/CVF Conference on Computer Vision and Pattern Recognition*, 4015–4024.
- Heusel, M.; Ramsauer, H.; Unterthiner, T.; Nessler, B.; and Hochreiter, S. 2017. GANs trained by a two time-scale update rule converge to a local nash equilibrium. In *Advances in Neural Information Processing Systems*, 6629–6640.
- Hore, A.; and Ziou, D. 2010. Image quality metrics: PSNR vs. SSIM. In *Proceedings of the International Conference on Pattern Recognition*, 2366–2369.
- Hu, E. J.; Shen, Y.; Wallis, P.; Allen-Zhu, Z.; Li, Y.; Wang, S.; Wang, L.; Chen, W.; et al. 2022. LoRA: Low-rank adaptation of large language models. In *Proceedings of the International Conference on Learning Representations*.
- Hu, L. 2024. Animate Anyone: Consistent and controllable image-to-video synthesis for character animation. In *Proceedings of the IEEE/CVF Conference on Computer Vision and Pattern Recognition*, 8153–8163.
- Kirillov, A.; Mintun, E.; Ravi, N.; Mao, H.; Rolland, C.; Gustafson, L.; Xiao, T.; Whitehead, S.; Berg, A. C.; Lo, W.-Y.; et al. 2023. Segment anything. In *Proceedings of the IEEE/CVF International Conference on Computer Vision*, 4015–4026.
- Liu, S.; Zeng, Z.; Ren, T.; Li, F.; Zhang, H.; Yang, J.; Jiang, Q.; Li, C.; Yang, J.; Su, H.; et al. 2024. Grounding dino: Marrying dino with grounded pre-training for open-set object detection. In *Proceedings of the European Conference on Computer Vision*, 38–55.
- MooreThreads. 2024. Moore-AnimateAnyone. <https://github.com/MooreThreads/Moore-AnimateAnyone>.
- Rombach, R.; Blattmann, A.; Lorenz, D.; Esser, P.; and Ommer, B. 2022. High-resolution image synthesis with latent diffusion models. In *Proceedings of the IEEE/CVF Conference on Computer Vision and Pattern Recognition*, 10684–10695.
- Ronneberger, O.; Fischer, P.; and Brox, T. 2015. U-Net: Convolutional networks for biomedical image segmentation. In *Proceedings of the Medical Image Computing and Computer-Assisted Intervention*, 234–241.
- Unterthiner, T.; Van Steenkiste, S.; Kurach, K.; Marinier, R.; Michalski, M.; and Gelly, S. 2018. Towards accurate generative models of video: A new metric & challenges. *arXiv preprint arXiv:1812.01717*.
- Wang, T.; Li, L.; Lin, K.; Zhai, Y.; Lin, C.-C.; Yang, Z.; Zhang, H.; Liu, Z.; and Wang, L. 2024. Disco: Disentangled control for realistic human dance generation. In *Proceedings of the IEEE/CVF Conference on Computer Vision and Pattern Recognition*, 9326–9336.
- Wang, Z.; Bovik, A. C.; Sheikh, H. R.; and Simoncelli, E. P. 2004. Image quality assessment: from error visibility to structural similarity. *IEEE Transactions on Image Processing*, 600–612.
- Wei, H.; Yang, Z.; and Wang, Z. 2024. Aniportrait: Audio-driven synthesis of photorealistic portrait animation. *arXiv preprint arXiv:2403.17694*.
- Xu, Z.; Zhang, J.; Liew, J. H.; Yan, H.; Liu, J.-W.; Zhang, C.; Feng, J.; and Shou, M. Z. 2024. MagicAnimate: Temporally consistent human image animation using diffusion model. In *Proceedings of the IEEE/CVF Conference on Computer Vision and Pattern Recognition*, 1481–1490.
- Yang, Z.; Zeng, A.; Yuan, C.; and Li, Y. 2023. Effective whole-body pose estimation with two-stages distillation. In *Proceedings of the IEEE/CVF International Conference on Computer Vision*, 4210–4220.
- Zablotskaia, P.; Siarohin, A.; Zhao, B.; and Sigal, L. 2019. Dwnet: Dense warp-based network for pose-guided human video generation. *arXiv preprint arXiv:1910.09139*.
- Zhang, L.; Rao, A.; and Agrawala, M. 2023. Adding conditional control to text-to-image diffusion models. In *Proceedings of the IEEE/CVF International Conference on Computer Vision*, 3836–3847.
- Zhang, R.; Isola, P.; Efros, A. A.; Shechtman, E.; and Wang, O. 2018. The unreasonable effectiveness of deep features as a perceptual metric. In *Proceedings of the IEEE/CVF Conference on Computer Vision and Pattern Recognition*, 586–595.
- Zhang, Y.; Gu, J.; Wang, L.-W.; Wang, H.; Cheng, J.; Zhu, Y.; and Zou, F. 2024. Mimicmotion: High-quality human motion video generation with confidence-aware pose guidance. *arXiv preprint arXiv:2406.19680*.
- Zhou, J.; Wang, M.; Li, T.; Meng, G.; and Chen, K. 2024. Dormant: Defending against Pose-driven Human Image Animation. *arXiv preprint arXiv:2409.14424*.

A More visualization Results

We provide more visualization results of **PoseGuard** based on full-parameter fine-tuning in Figure 11, covering various unsafe poses (e.g., discriminatory, NSFW) as well as any other poses¹ that the defender intends to guard against. The visualizations showcase our method’s ability to effectively defend against a wide range of poses, causing the generation quality to severely degrade into either nearly black outputs or heavily distorted images. These results further demonstrate the strong pose capacity and defense effectiveness of **PoseGuard**.

B Results of Continuous Pose Sequences

Figure 12 shows more results of continuously varying pose sequences, demonstrating **PoseGuard**’s ability to handle transitional frames with unsafe poses embedded within otherwise normal pose sequences.

C Unsafe Pose Dataset

Figure 13 shows examples of the 50 unsafe poses collected in our dataset. The full collection is available upon request for research purposes, subject to ethical review.

D Safe Output Target Selection

We compare black versus blurred images as safe targets. Blurred images better preserve benign visual quality while maintaining strong suppression, as shown in Table 6. This offers a flexible trade-off between defense strength and perceptual fidelity.

E Fine-Tuned Module Selection

Table 7 shows that fine-tuning both Denoising UNet and Reference UNet brings no notable gains over tuning only the Denoising UNet. We therefore adopt Denoising UNet fine-tuning to achieve strong defense with minimal parameter overhead.

¹The poses used in this experiment are collected from an open-source platform Civitai.

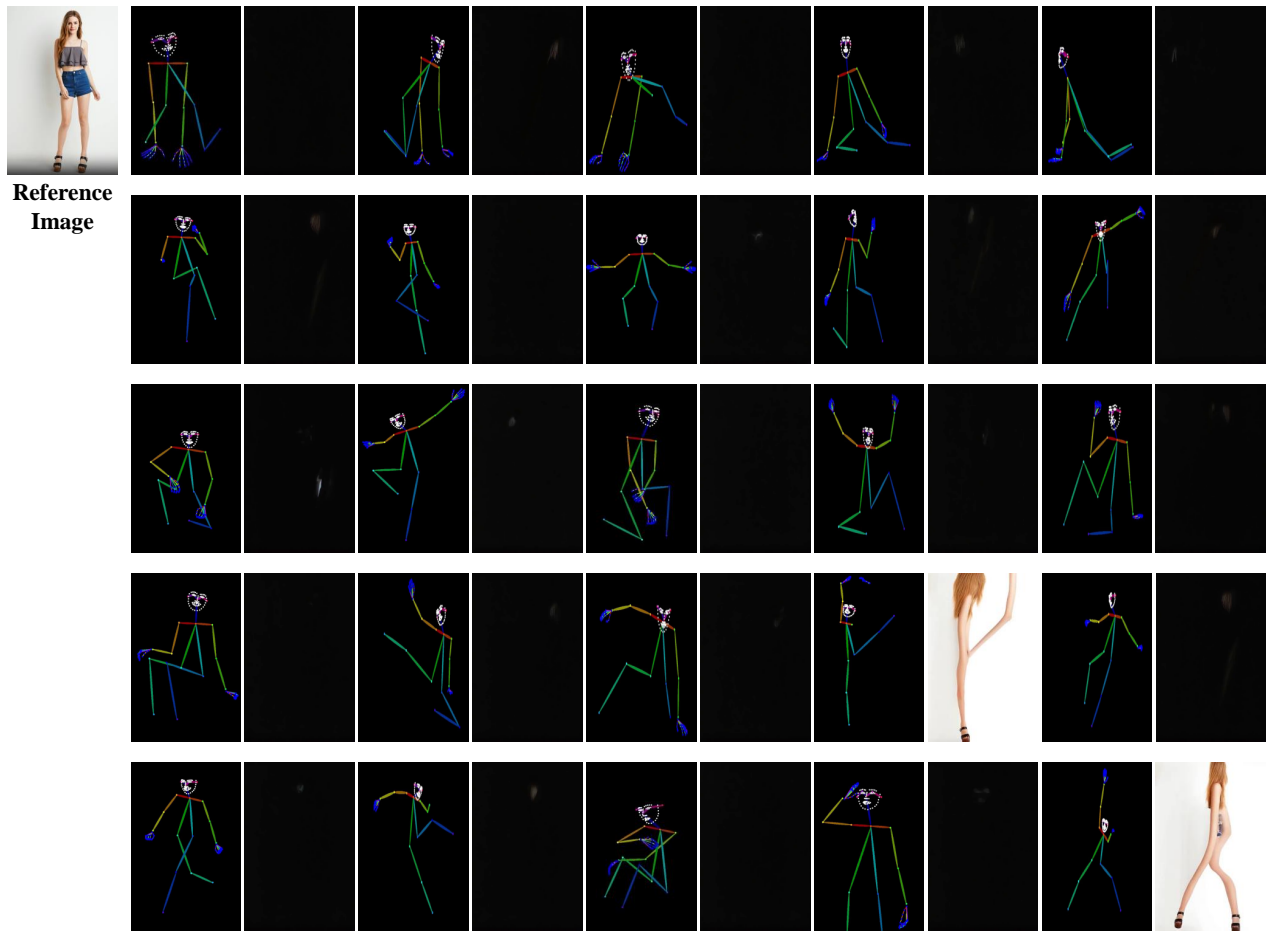


Figure 11: More Visualized Results of Full-parameter Fine-tuning.

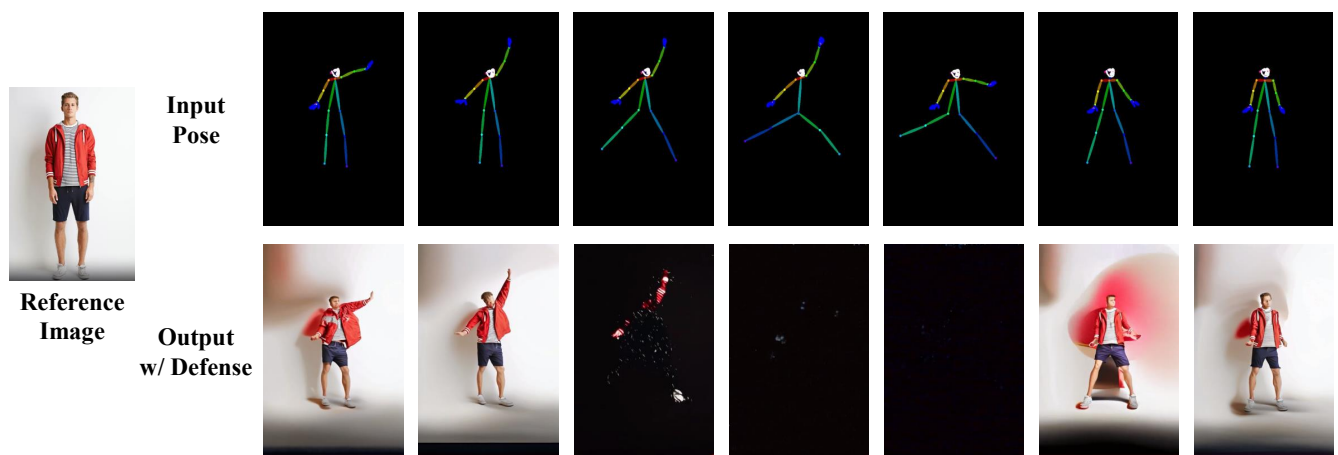


Figure 12: Results of continuous pose sequences.

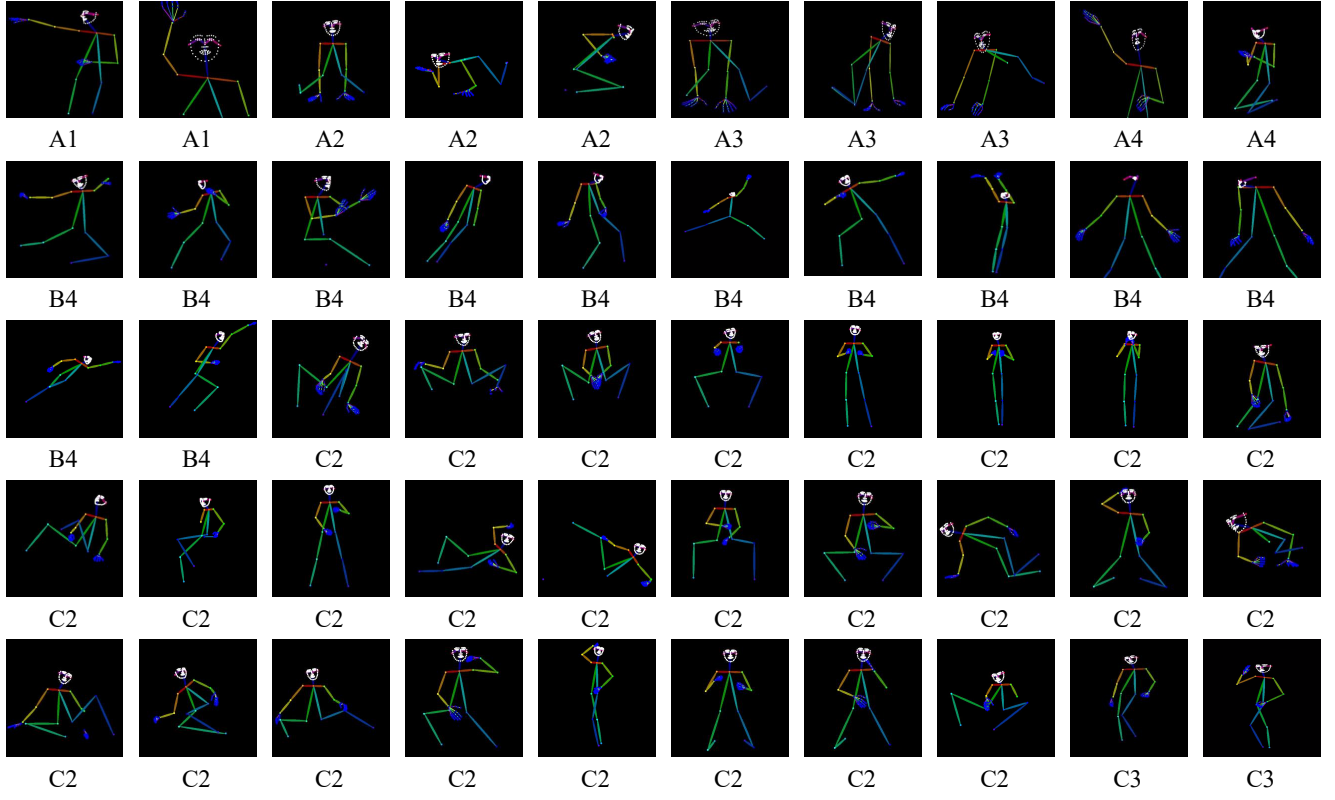


Figure 13: Examples of the 50 unsafe poses collected in our dataset. The poses are categorized into three categories: (A) Discriminatory pose, (B) Copyright-sensitive pose, and (C) NSFW pose. They are sourced from multiple online platforms, including (1) Wikipedia, (2) Render-State, (3) Civitai, and (4) Google Search.

Method	Generation Quality Metrics						Defense Metrics			
	FID-VID ↓	FVD ↓	FID ↓	SSIM ↑	PSNR ↑	LPIPS ↓	SSIM* ↓	PSNR* ↓	LPIPS* ↑	PSR ↑
LoRA-FT-4	7.842	231.10	31.863	0.88406	35.362	0.09740	0.79002	30.083	0.32498	1.000
LoRA-FT-8	12.800	278.77	43.752	0.87700	35.065	0.11023	0.79844	30.299	0.28938	0.958
LoRA-FT-16	19.690	327.40	60.563	0.86454	34.611	0.14182	0.77764	30.087	0.32567	0.980
LoRA-FT-32	18.974	292.13	54.128	0.86880	34.862	0.12998	0.76522	29.881	0.34330	0.980

Table 6: Results of using a blurred reference image as target safe output. LoRA-FT- n denotes LoRA fine-tuning on n unsafe poses.

Method	Generation Quality Metrics						Defense Metrics		
	FID-VID ↓	FVD ↓	FID ↓	SSIM ↑	PSNR ↑	LPIPS ↓	SSIM* ↓	PSNR* ↓	LPIPS* ↑
FT-D	18.750	281.71	28.957	0.87972	36.161	0.09418	0.06103	27.551	0.53305
FT-DR	13.342	338.72	26.284	0.87760	35.511	0.08631	0.21349	27.719	0.55615

Table 7: Impact of fine-tuned modules on defense performance, under the setting of full-parameter fine-tuning with four poses while keeping all other parameters fixed. FT-D denotes fine-tuning Denoising UNet. FT-DR denotes fine-tuning Denoising UNet and Reference UNet.